Hindawi
Advances in Civil Engineering
Volume 2023, Article ID 6733848, 7 pages
https://doi.org/10.1155/2023/6733848

Research Article

Breaking Undular and Breaking Surges Advancing in Still Water

Feidong Zheng[1] **and Xueyi Li**[2]

[1]*PowerChina Kunming Engineering Corporation Limited, Kunming 650051, China*
[2]*College of River and Ocean Engineering, Chongqing Jiaotong University, Chongqing 400074, China*

Correspondence should be addressed to Xueyi Li; xy_lee@cqjtu.edu.cn

Received 2 February 2023; Revised 2 April 2023; Accepted 14 June 2023; Published 28 June 2023

Academic Editor: Iacopo Carnacina

The propagation of secondary surges can lead to unexpected interaction events with navigation ships and downstream hydraulic structures; hence, they may cause navigation accidents and structural damage. In the present study, physical experiments were performed in a long water wave tank to study the evolution of breaking undular and breaking surges advancing in still water. Both free-surface and velocity measurements were conducted. It was observed that the transition from a breaking undular surge to a breaking surge occurred as the ratio of the mean water depth behind the surge to the still water depth equal to 1.68–1.71. Empirical expressions based on the experimental data were proposed to predict the wave amplitude and wave steepness of breaking undular surges. The unsteady flow results demonstrated that the normalized longitudinal velocity component beneath the surge front was governed mainly by the normalized free-surface elevation, independently of the surge type. Moreover, the maximum vertical velocity component during the surge front passage had a linear dependence on the vertical location. The present result provided new quantitative information on breaking undular and breaking surges advancing in still water.

1. Introduction

Three types of secondary surges can develop at the wave face of a long wave: nonbreaking undular surge, breaking undular surge, and breaking surge [1]. Such surges can be observed in shallow water conditions when a tide wave enters a converging river [2] or after the operation of lock chambers in a navigation channel [3]. Secondary surges can also occur in intermediate or deep water conditions during the nonlinear evolution process of long-crested wave groups [4]. The generation and development of secondary surges results from imbalance between wave nonlinearity and dispersion effects [5–7]. These surges have a great impact on the ecology and estuarine processes [8, 9]. The propagation of secondary surges may lead to extreme interaction events with coastal and marine structures, compromising the stability of these structures, and even causing loss of structural functionality [4, 10–12]. In navigation channels, secondary surges can also impose violent impact loads on navigation ships and downstream hydraulic structures (e.g., lock gates, sluices, and dams), causing navigation accidents and structural damage [13]. Therefore, quantitative characterization of the nonlinear evolution of secondary surges is important for evaluating potential damages to infrastructure and navigation ships.

Because of the potential impact caused by secondary surges, the mechanisms governing their evolution have been widely investigated. Most of previous investigations have focused on secondary surges propagating against an initially steady flow, such as Chanson [14], Gualtieri and Chanson [15, 16], Docherty and Chanson [17], Simon [18], and Leng and Chanson [19]. According to these studies, the following important conclusions were drawn. First, the transition from a nonbreaking undular surge to a breaking one depended on the surge Froude number and the degree of the boundary layer development at the toe of the surge. Second, the wave parameters (i.e., wave amplitude, wavelength, and wave steepness) and the wave shape of an undular surge could not be accurately predicted using existing solutions derived from linear wave theory and the Boussinesq equations, independently of the surge type. Third, the streamwise velocity component exhibited an oscillating feature with maximum and minimum velocities obtained beneath the wave troughs and crests of an undular surge, respectively. Fourth, the

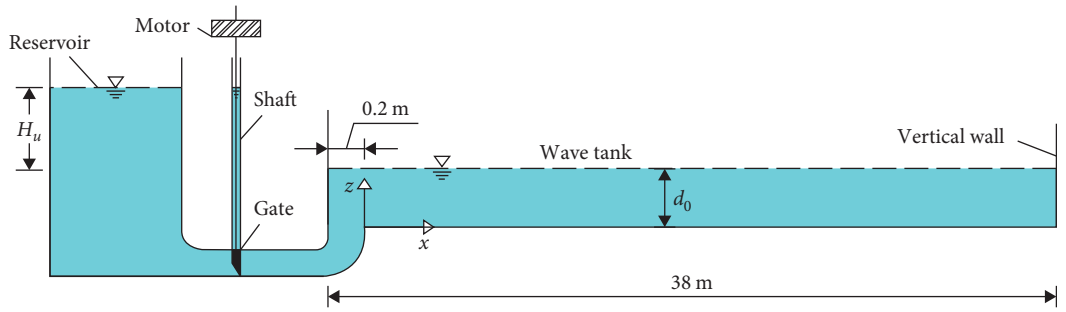

Figure 1: Sketch of the experimental arrangement.

Table 1: Details of free surface and velocity measurements.

Measurements	d_0 (m)	t_v (s)	H_u (m)	Instrumentation location x (m)	z/h_0
Free surface	0.08	20	0.2–0.5	3–36	/
Velocity	0.08	20	0.4	15–30	0.08–0.91

largest turbulent Reynolds stress components occurred beneath the wave crests of an undular surge in the absence of flow reversal induced by the surge. A different insight into the flow structures beneath both nonbreaking undular and breaking surges was obtained by considering the Kolmogorov complexity [20]. This has demonstrated a marked effect of an undular surge passage on the vertical distribution of the Kolmogorov complexity for the streamwise velocity, which was not influenced by a breaking surge passage. Recently, a new analytic solution has been developed based on the potential wave theory by Chen et al. [21] to describe the wave feature of nonbreaking undular surges propagating against a steady flow. The comparison between the proposed analytic solution and experimental results indicated that both the wave amplitude and wave celerity were well reproduced. In contrast, the study of the evolution of secondary surges in still water has received less attention except a few investigations (e.g., Peregrine [22], Hornung et al. [23], and Lin et al. [24]). In fact, the wave features of secondary surges were highly dependent upon the initial flow conditions prior to surge arrival (i.e., still water and steady flow), which has been demonstrated by Benet and Cunge [25], and Zheng et al. [26]. There are indeed fundamental differences between the two types of secondary surge flows.

Recently, the nonlinear evolution of nonbreaking undular surges advancing in still water has been systematically investigated by Zheng et al. [27]. Their results indicated that the leading wave front of a nonbreaking undular surge was close to that of a solitary wave in shallow water region during the entire wave evolution process. This finding obtained for nonbreaking undular surges encourage further quantitative investigation of breaking undular and breaking surges advancing in still water as well. The mechanisms governing the free-surface dynamics and velocity distributions of breaking undular and breaking surges are not yet well understood. However, detailed investigation on these aspects is inevitable for understanding the overall evolution process of secondary surges advancing in still water. In addition, the requirement for datasets for the validation of the corresponding numerical models developed for breaking undular and breaking undular surges advancing in still water remains imperative.

To date, limited quantitative information is available on the evolution characteristics of breaking undular and breaking surges advancing in still water. The study presents such an investigation, which was performed in a long water wave tank. This paper is organized as follows. The experimental methodology is presented in Section 2. In Section 3, the transition from a breaking undular surge to a breaking surge is first identified. The wave features of breaking undular surges are subsequently investigated. The velocity distributions beneath two types of secondary surges are further analyzed and discussed. Finally, conclusions of this study are drawn in Section 4.

2. Experimental Setup and Experiments

A schematic description of the experiment setup is shown in Figure 1. The details of the experimental arrangement can be found in Zheng et al. [27], and a brief description is provided here. The experiments were carried out in a rectangular horizontal wave tank, which was 0.3 m wide, 0.35 m deep, and 38 m long. The tank was made of plexiglass walls and a smooth polyvinyl chloride bed. A vertical wall was placed at right angle to the direction of surge propagation. The tank was connected to a reservoir (1×1 m in plane xy) through a pipe, which was equipped with a plate gate and the corresponding shaft. In the current study, the still water depth d_0 and the gate lifting time t_v were fixed at 0.08 m and 20 s, respectively. The only variable determining the development process of a surge was the drop height H_u. The details of the experiments are listed in Table 1. Overall, four different drop heights ranging from $H_u = 0.2$–0.5 m were tested. When lifting the gate at $t_v = 20$ s, a nonbreaking undular surge induced by water flow in the tank was first observed. During wave propagation, the nonbreaking undular surge exhibited significant wave amplification and subsequently evolved into a breaking undular surge. This process

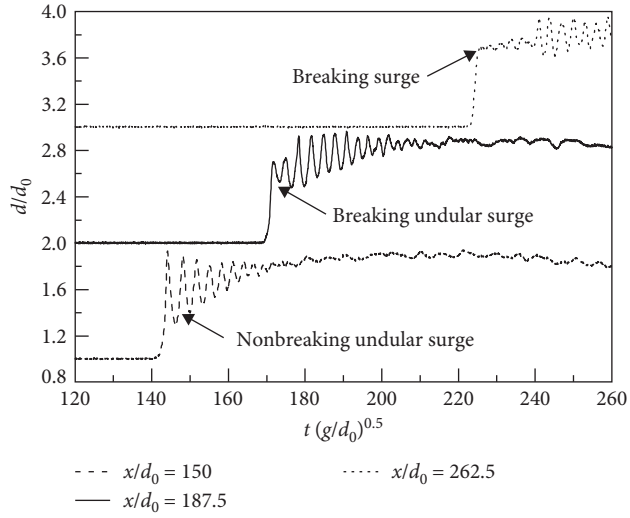

Figure 2: Temporal evolution of wave profiles.

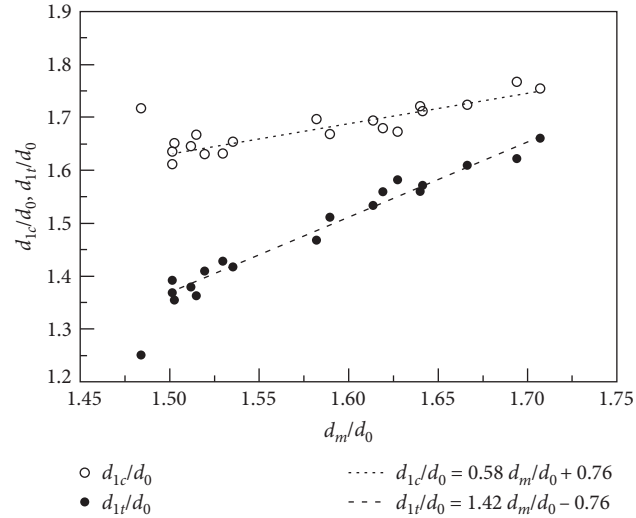

Figure 3: Normalized water depths d_{1c}/d_0 and d_{1t}/d_0 as functions of d_m/d_0.

was observed in all experiments. For some experiments (i.e., $H_u \geq 0.4$ m), the breaking undular surge transferred to the breaking surge regime. The present research focused on the evolution of breaking undular and breaking surges. Each experiment was stopped when the leading wave arrived at the vertical wall. The (x, z) coordinate system was chosen with the vertical upward pointing z-axis and the horizontal x-axis coinciding with the tank bed $z = 0$.

The free-surface features and velocity distributions of secondary surges were measured using a set of wave gauges and an acoustic Doppler velocimeter Nortek™ Vectrino+, respectively, with a sampling frequency of 200 Hz. The wave probes were located from $x = 3$ to 36 m with an interval of 3 m between two neighbor probes. The accuracy of the wave probes was 0.1 mm. Unsteady velocity measurements were performed at $x = 15$ and 30 m for one experiment with $H_u = 0.4$ m. The secondary surge was a breaking undular type at $x = 15$ m, whereas it was in the breaking surge region at $x = 30$ m. For each longitudinal location x, instantaneous velocity data at five vertical elevations (i.e., $z/d_0 = 0.08$, 0.13, 0.41, 0.71, and 0.91) were recorded with an accuracy of 1 cm/s. In the present study, tap water was used. The reservoir water was seeded with some vegetable dye to improve the quality and accuracy of the velocity data during instantaneous velocity measurements.

3. Results and Discussion

3.1. Flow Patterns. The temporal evolution of wave profiles at different longitudinal locations is shown in Figure 2, where the water depth d was normalized with d_0, and the time t was normalized with $(d_0/g)^{0.5}$ with g denoting the gravitational acceleration. Note that, the wave profile immediately prior to wave breaking at the leading wave crest (i.e., a nonbreaking undular surge at $x/d_0 = 150$) is also shown for comparison. It can be seen that the wave amplitude of an undular surge exhibited a sharp decrease shortly after the appearance of some wave breaking (i.e., a breaking undular surge at $x/d_0 = 187.5$). Over a large propagation distance (e.g., $x/d_0 = 262.5$), the free-surface undulations eventually disappeared and the breaking undular surge transferred to a breaking surge.

Pertaining to secondary surges propagating against an initially steady flow, the transition from a breaking undular surge to a breaking surge was usually characterized by the transition surge Froude number, e.g., Chanson [14] and Gualtieri and Chanson [15, 16]. However, a combined analysis of the results from these studies indicated that the transition surge Froude number was closely dependent on the inflow velocity. This revealed that the surge Froude number might not be a suitable index of transition flow conditions. Recently, the change in wave regime for secondary surges propagating against an initially steady flow was considered by Pelinovsky et al. [1]. Their results revealed that the surge type could be simply identified by the ratio of the mean water depth behind the surge front, d_m, to the still water depth. The same concept was applied herein to secondary surges advancing in still water. Note that the mean water depth was defined as the average of the water depths at the leading wave crest d_{1c}, and trough d_{1t}, for undular surges, whereas it referred to the water depth measured immediately after the surge front for breaking surges [28]. The present data showed that breaking undular surges occurred for $1.48 \leq d_m/d_0 \leq 1.71$, whereas breaking surges were observed for $1.68 \leq d_m/d_0 \leq 1.89$. Thus, criterion $d_m/d_0 = 1.68$–1.71 can be used as an estimate of the change in surge regime. It is worth noting that this criterion seems also valid for secondary surges propagating against an initially steady flow in field situations [1].

3.2. Wave Features of Breaking Undular Surges

3.2.1. Water Depths at the Leading Wave Crest and Trough. The variations of the normalized water depths at the leading wave crest and trough with d_m/d_0 during surge evolution are illustrated in Figure 3. It is clearly seen that the values of d_{1c}/d_0 and d_{1t}/d_0 for $d_m/d_0 = 1.48$ (these data were collected at $x = 18$ m, which was very close to the breaking location, i.e., $x = 17.2$ m) deviated significantly from the remaining data.

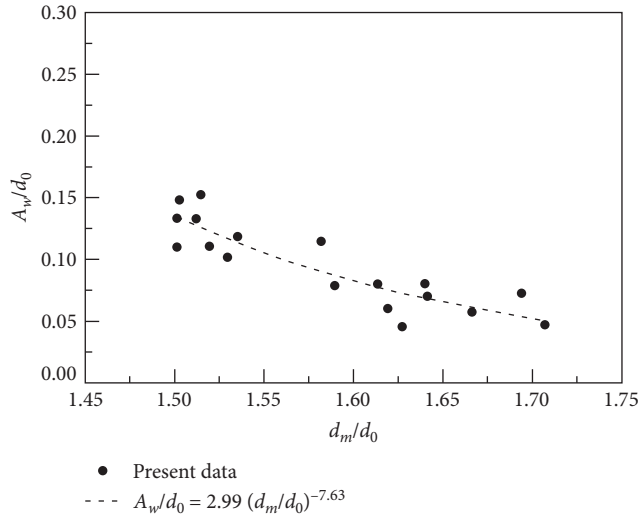

FIGURE 4: Normalized wave amplitude A_w/d_0 versus d_m/d_0.

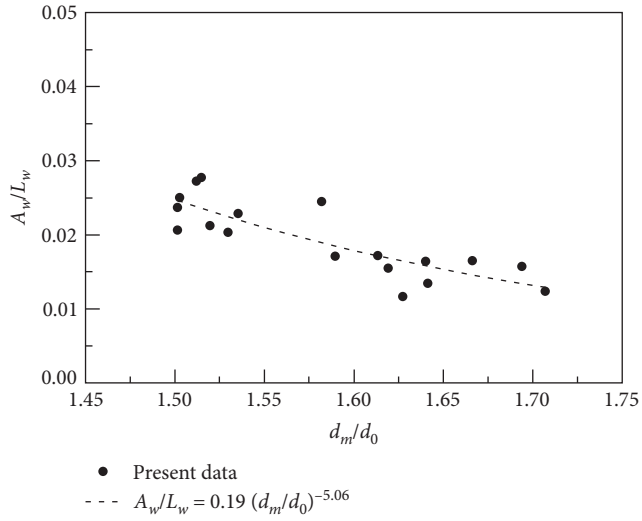

FIGURE 5: Wave steepness A_w/L_w versus d_m/d_0.

This discrepancy was attributed to the water depth redistribution process at the leading wave induced by wave breaking; therefore, the wave form for $d_m/d_0 = 1.48$ was instable. To ensure that this different behavior is fully declared, the measured data corresponding to $d_m/d_0 = 1.48$ are excluded in subsequent analyses. As d_m/d_0 increased, both d_{1c}/d_0 and d_{1t}/d_0 exhibited linearly increasing trends. In the experimental range of $1.50 \le d_m/d_0 \le 1.71$, the evolution of d_{1c}/d_0 and d_{1t}/d_0 could be related to the normalized mean water depth by

$$\frac{d_{1c}}{d_0} = 0.58\frac{d_m}{d_0} + 0.76, \tag{1}$$

$$\frac{d_{1t}}{d_0} = 1.42\frac{d_m}{d_0} - 0.76, \tag{2}$$

with a correlation coefficient $r^2 = 0.85$ and 0.97 for Equations (1) and (2), respectively.

3.2.2. Wave Amplitude and Steepness. In undular surges, the wave amplitude A_w was defined as half of the difference between the water depths at the leading wave crest and trough. The wavelength, L_w, referred to the distance between the first and second wave crests. The dominant influence of the normalized mean depth d_m/d_0 on the wave amplitude is shown in Figure 4. It was expected that the wave amplitude decayed with increasing d_m/d_0. In the range $1.50 \le d_m/d_0 \le 1.71$, the variation of A_w/d_0 during surge evolution could be described by

$$\frac{A_w}{d_0} = 2.99\left(\frac{d_m}{d_0}\right)^{-7.63}, \tag{3}$$

with a correlation coefficient $r^2 = 0.78$.

The dependency of the wave steepness on the normalized water depth is presented in Figure 5. A decrease in the wave steepness with increasing d_m/d_0 was clearly observed. The experimental data suggested a relationship between A_w/L_w and d_m/d_0

$$\frac{A_w}{L_w} = 0.19\left(\frac{d_m}{d_0}\right)^{-5.06}, \tag{4}$$

with a correlation coefficient of 0.68.

3.3. Velocity Field beneath Advancing Surges

3.3.1. Temporal Evolution of Velocity Components. Figures 6(a) and 6(b) illustrate the effects of a breaking undular surge and a breaking surge on velocity field. In each graph, the variations of $V_x/(gd_0)^{0.5}$, $V_y/(gd_0)^{0.5}$, $V_z/(gd_0)^{0.5}$, and d/d_0 were plotted against the normalized time relative to the first maximum elevation of the water surface, $(t-t_0)(g/d_0)^{0.5}$.The experimental data highlighted the rapid increase of the streamwise velocity component during the surge front passage. The $V_x/(gd_0)^{0.5}$ oscillated with the free-surface undulations behind the breaking undular surge front, while it was almost constant after the breaking surge front. Note that for all experiments, a short time lag was observed between the first maximum elevation of the water surface and the maximum longitudinal velocity component. During the passage of the breaking undular surge, the transverse velocity component showed some irregular fluctuations. In contrast, the $V_y/(gd_0)^{0.5}$ exhibited a larger fluctuation range associated with some low frequency pattern during the breaking surge passage. The experimental data from Koch and Chanson [28] demonstrated a similar behavior of the transverse velocity component in a breaking surge propagating against an initially steady flow. For both types of surges, the vertical velocity component reached its maximum value, V_{zm}, beneath the surge front.

3.3.2. Velocity Distributions beneath Surge Fronts. The numerical results of Zheng and Li [13] showed that the depth-averaged longitudinal velocity component beneath the surge front of a nonbreaking undular surge was close to that of a solitary wave in shallow water region [29]. Herein, a quantitative investigation on the longitudinal velocity component

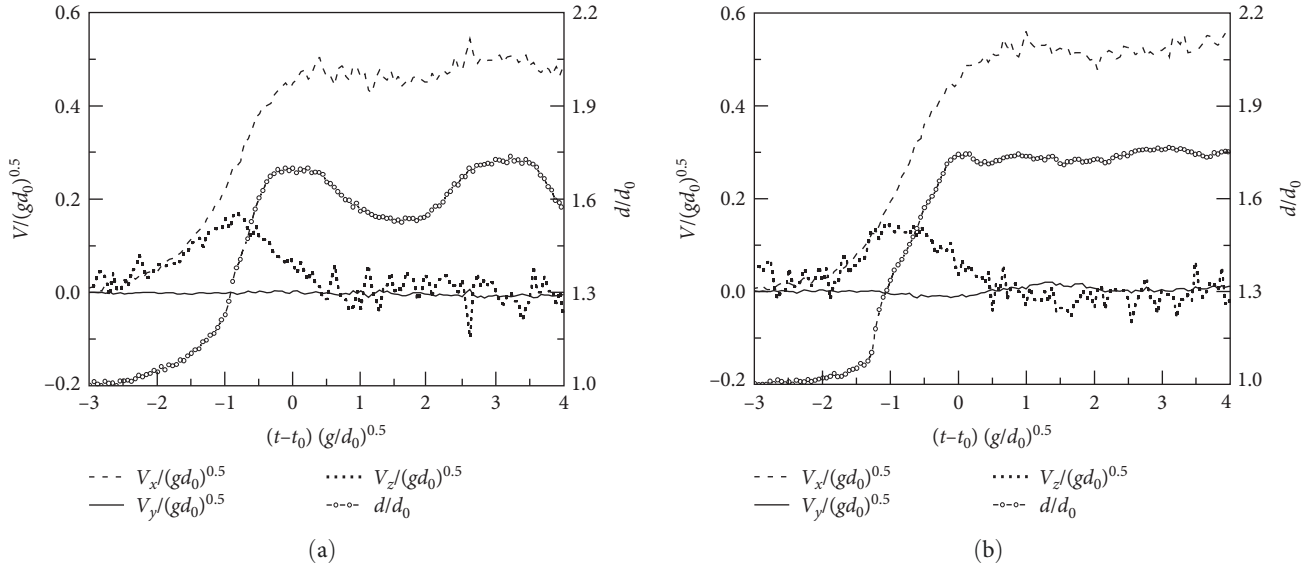

FIGURE 6: Instantaneous velocity components induced by surges ($z/d_0 = 0.71$):; (a) breaking undular surge, $d_m/d_0 = 1.61$and (b) breaking surge, $d_m/d_0 = 1.74$.

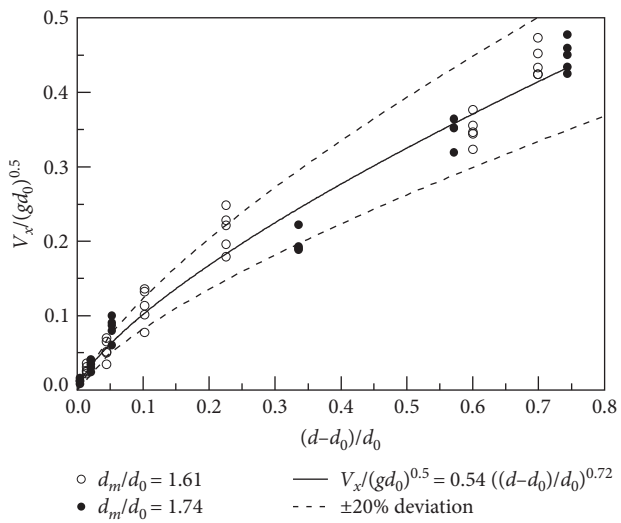

FIGURE 7: $V_x/(gd_0)^{0.5}$ versus $(d-d_0)/d_0$ for breaking undular and breaking surges.

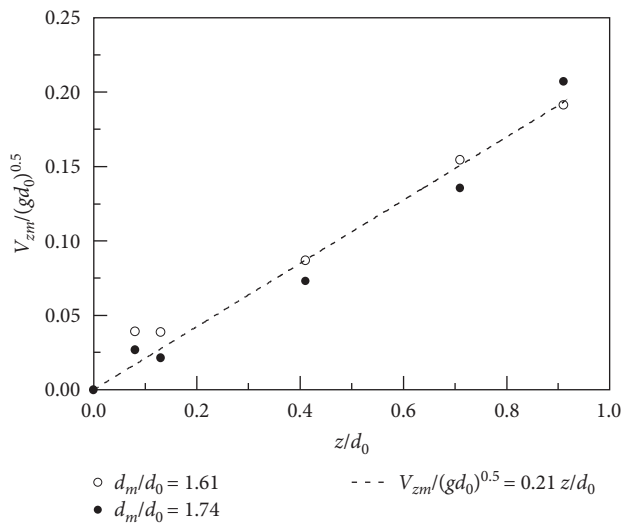

FIGURE 8: $V_{zm}/(gd_0)^{0.5}$ versus z/d_0 for breaking undular and breaking surges.

distributions beneath the surge fronts of the breaking undular and breaking surges was carried out. For each vertical location z, instantaneous velocity data at several representative moments (i.e., $(t-t_0)/(g/d_0)^{0.5} = 0$, -0.5, -1.0, -1.5, -2.0, and -2.5) were extracted. The dependance of the normalized longitudinal velocity component beneath the surge fronts on $(d-d_0)/d_0$ is shown in Figure 7. The relation between $V_x/(gd_0)^{0.5}$ and $(d-d_0)/d_0$ for two types of surges was well described by the following equation

$$\frac{V_x}{\sqrt{gd_0}} = 0.54\left(\frac{d-d_0}{d_0}\right)^{0.72}, \tag{5}$$

with a deviation of ±20% and a correlation coefficient of 0.97. This finding revealed that the normalized longitudinal velocity component distributions beneath the surge fronts exhibited a similar trend to that predicted by the second-order solitary wave solution derived by Laitone [29].

Figure 8 shows the variation of the maximum vertical velocity component along the water column. Note that the vertical velocity component was null at the impervious tank bed. A linear distribution of the maximum vertical velocity component was observed during the surge front passage for both breaking undular and breaking surges. This finding was in agreement with the earlier observation of Docherty and Chanson [17], although they studied the velocity distribution induced by a breaking surge propagating against an initially steady flow. It is noteworthy that the linear distribution of the maximum vertical velocity component was consistent with Boussinesq's approximation for a solitary wave [30].

4. Conclusions

In this study, the evolution of breaking undular and breaking surges advancing in still water was physically investigated in a series of experiments conducted in a long water wave channel, extending a previous study by Zheng et al. [27]. The main findings are summarized as follows.

A breaking undular surge was observed for the relative mean water depth behind the surge front d_m/d_0 in the range from 1.48 to 1.71, whereas a breaking surge occurred for $1.68 \leq d_m/d_0 \leq 1.89$. The change in surge regime could be approximated as $d_m/d_0 = 1.68$–1.71, which was close to the transition criterion for secondary surges propagating against an initially steady flow [1], indicating a negligible effect of the initial flow conditions on the transition of the surge types. Pertaining to breaking undular surges, the water depths at the leading wave crest and trough exhibited linear increasing trends with increasing d_m/d_0, whereas the distributions of wave amplitude and steepness followed a power law. For both breaking undular and breaking surges, the longitudinal velocity component beneath the surge front depended primarily on the free-surface elevation. Moreover, the maximum vertical velocity component presented a linear distribution along the water column, coinciding with Boussinesq's approximation. This study provided new quantitative results on the evolution characteristics of breaking undular and breaking surges advancing in still water, which might be used to validate numerical models for secondary surge evolution.

Data Availability

The data used to support the findings of this study are available from the corresponding author upon request.

Conflicts of Interest

The authors declare that they have no conflicts of interest.

Acknowledgments

This study was supported by the China Postdoctoral Science Foundation (grant no. 2021M700620); Natural Science Foundation of Chongqing, China (grant no. cstc2021jcyj-bshX0049).

References

[1] E. N. Pelinovsky, E. G. Shurgalina, and A. A. Rodin, "Criteria for the transition from a breaking bore to an undular bore," *Izvestiya, Atmospheric and Oceanic Physics*, vol. 51, pp. 530–533, 2015.

[2] X. Leng, "*A study of turbulence: the unsteady propagation of bores and surges*," Ph.D. Thesis, The University of Queensland, Brisbane, 2018.

[3] A. Treske, "Undular bores (favre-waves) in open channels—experimental studies," *Journal of Hydraulic Research*, vol. 32, no. 3, pp. 355–370, 1994.

[4] G. Akrish, O. Rabinovitch, and Y. Agnon, "Extreme run-up events on a vertical wall due to nonlinear evolution of incident wave groups," *Journal of Fluid Mechanics*, vol. 797, pp. 644–664, 2016.

[5] O. Castro-Orgaz and H. Chanson, "Undular and broken surges in dam-break flows: a review of wave breaking strategies in a Boussinesq-type framework," *Environmental Fluid Mechanics*, vol. 20, pp. 1383–1416, 2020.

[6] S. S. Frazao and Y. Zech, "Undular bores and secondary waves—Experiments and hybrid finite-volume modelling," *Journal of Hydraulic Research*, vol. 40, no. 1, pp. 33–43, 2002.

[7] O. Kurkina and E. Pelinovsky, "Nonlinear transformation of sine wave within the framework of symmetric (2+4) KdV equation," *Symmetry*, vol. 14, no. 4, Article ID 668, 2022.

[8] C. Donnelly and H. Chanson, "Environmental impact of undular tidal bores in tropical rivers," *Environmental Fluid Mechanics*, vol. 5, pp. 481–494, 2005.

[9] F. N. Cantero-Chinchilla, R. J. Bergillos, P. Gamero, O. Castro-Orgaz, L. Cea, and W. H. Hager, "Vertically averaged and moment equations for dam-break wave modeling: shallow water hypotheses," *Water*, vol. 12, no. 11, Article ID 3232, 2020.

[10] F. Carbone, D. Dutykh, J. M. Dudley, and F. Dias, "Extreme wave runup on a vertical cliff," *Geophysical Research Letters*, vol. 40, no. 12, pp. 3138–3143, 2013.

[11] C. Viotti, F. Carbone, and F. Dias, "Conditions for extreme wave runup on a vertical barrier by nonlinear dispersion," *Journal of Fluid Mechanics*, vol. 748, pp. 768–788, 2014.

[12] G. Akrish, R. Schwartz, O. Rabinovitch, and Y. Agnon, "Impact of extreme waves on a vertical wall," *Natural Hazards*, vol. 84, no. S2, pp. 637–653, 2016.

[13] F. Zheng and X. Li, "Undular surges interaction with a vertical wall," *Marine Georesources & Geotechnology*, vol. 40, no. 10, pp. 1224–1231, 2022.

[14] H. Chanson, "Undular tidal bores: basic theory and free-surface characteristics," *Journal of Hydraulic Engineering*, vol. 136, no. 11, pp. 940–944, 2010.

[15] C. Gualtieri and H. Chanson, "Experimental study of a positive surge. Part 1: basic flow patterns and wave attenuation," *Environmental Fluid Mechanics*, vol. 12, pp. 145–159, 2012.

[16] C. Gualtieri and H. Chanson, "Experimental study of a positive surge. Part 2: comparison with literature theories and unsteady flow field analysis," *Environmental Fluid Mechanics*, vol. 11, pp. 641–651, 2011.

[17] N. J. Docherty and H. Chanson, "Physical modeling of unsteady turbulence in breaking tidal bores," *Journal of Hydraulic Engineering*, vol. 138, no. 5, pp. 412–419, 2012.

[18] B. Simon, "*Effects of tidal bores on turbulent mixing: a numerical and physical study in positive surges*," Ph.D. Thesis, The University of Queensland, Brisbane, 2013.

[19] X. Leng and H. Chanson, "Breaking bore: physical observations of roller characteristics," *Mechanics Research Communications*, vol. 65, pp. 24–29, 2015.

[20] C. Gualtieri, A. Mihailović, and D. Mihailović, "An application of Kolmogorov complexity and its spectrum to positive surges," *Fluids*, vol. 7, no. 5, Article ID 162, 2022.

[21] C.-T. Chen, J.-F. Lee, H. Chanson, K.-T. Lin, and C.-J. Lin, "A time-domain analytic solution of flow-induced undular bores," *Journal of Marine Science and Engineering*, vol. 10, no. 6, Article ID 738, 2022.

[22] D. H. Peregrine, "Calculations of the development of an undular bore," *Journal of Fluid Mechanics*, vol. 25, no. 2, pp. 321–330, 1966.

[23] H. G. Hornung, C. Willert, and S. Turner, "The flow field downstream of a hydraulic jump," *Journal of Fluid Mechanics*, vol. 287, pp. 299–316, 1995.

[24] C. Lin, W.-Y. Wong, M.-J. Kao, J. Yang, R. V. Raikar, and J.-M. Yuan, "Hydrodynamic features of an undular bore

traveling on a 1:20 sloping beach," *Water*, vol. 11, no. 8, Article ID 1556, 2019.
[25] F. Benet and J. A. Cunge, "Analysis of experiments on secondary undulations caused by surge waves in trapezoidal channels," *Journal of Hydraulic Research*, vol. 9, no. 1, pp. 11–33, 1971.
[26] F. Zheng, P. Wang, J. An, and Y. Li, "Characteristics of undular surges propagating in still water," *KSCE Journal of Civil Engineering*, vol. 25, pp. 3359–3368, 2021.
[27] F. Zheng, P. Wang, M. Wang, and J. Zhang, "The evolution and runup of nonbreaking undular surges," *Marine Georesources & Geotechnology*, vol. 40, no. 7, pp. 774–781, 2022.
[28] C. Koch and H. Chanson, *An Experimental Study of Tidal Bores and Positive Surges: Hydrodynamics and Turbulence of the Bore Front*, The University of Queensland, Brisbane, 2005.
[29] E. V. Laitone, "The second approximation to cnoidal and solitary waves," *Journal of Fluid Mechanics*, vol. 9, no. 3, pp. 430–444, 1960.
[30] J. V. Boussinesq, "Sur le mouvement permanent varié de l'eau dans les tuyaux de conduite et dans les canaux découverts," *Comptes Rendus des Séances de l'Académie des Sciences*, vol. 73, pp. 101–105, 1871.